Analysis of the Interaction between Jet and Plume Flows of a Light Gas with an Extended Ceiling Based on the Results of Experimental Studies

Denisenko V.P.[1], Kirillov I.A.[1], Korobtsev S.V.[1], Nikolaev I.I.[1],*, Bystrov P.A.[2]

[1] *NRC "Kurchatov Institute", Russian Federation*
[2] *IPCE RAS, Russian Federation*
**Corresponding author's email:* hitcliff68@mail.ru

ABSTRACT

The study is devoted to the generalization of the experimental results obtained by means of investigation of the quantitative characteristics of the modeled flammable hydrogen-air cloud which can occur in case of emergency leaks of hydrogen in underground or multi-story parking lots of hydrogen transport. Data are presented on 28 runs of light helium gas (hydrogen substitute) during its vertical propagation and interaction with an extended ceiling in case of two main types of outflow - jet and plume. The analysis of the experimental data by varying the parameters of helium release revealed different types of asymptotic decline of helium concentration in the under-ceiling layer along the radius of spreading, as well as different behavior of the under-ceiling layer thickness. The consequence of this difference was that, in the case of plume outflow, much larger volumes of the simulated fire-hazardous mixture were observed in the under-ceiling layer than in case of jet outflows. Some qualitative analytical explanation of the observed phenomena was proposed, that could be used to establish quantitative theoretical dependencies useful for development of the engineering guidelines on safety of the semi-confined and confined parking areas for hydrogen-fueled vehicles.

KEYWORDS: Hydrogen leak, plume and jet flow, flammable volume, under-ceiling layer.

INTRODUCTION

The main features of the distribution of hydrogen-air mixtures in confined spaces (ventilated and unventilated rooms of nuclear power plants, individual garages or repair shops) where the vertical and horizontal dimensions of the premises are commensurate with each other have been intensively studied recently [1-6]. Specific features and engineering relations for the case of formation of flammable hydrogen-air volumes in non-ventilated, semi-confined spaces are currently in the stage of preliminary studies. A typical example of a semi-confined space is the underground parking of vehicles using light combustible gas (hydrogen, methane), where the ceiling height is much less than the width and length of the parking hall.

This experimental study is devoted to the modeling of vertical leakage of light gas-helium (as hydrogen surrogate) under conditions simulating the outflow of hydrogen under an extended ceiling. A detailed study of the main features of the interaction of light floating gas with the horizontal surface of the ceiling in a semi–confined room in two main modes of vertical outflow - jet and plume - was carried out using a specially developed multipoint system for measuring helium concentrations in real time.

Proceedings of the Ninth International Seminar on Fire and Explosion Hazards (ISFEH9), pp. 1335-1347
Edited by Snegirev A., Liu N.A., Tamanini F., Bradley D., Molkov V., and Chaumeix N.
Published by Saint-Petersburg Polytechnic University Press
ISBN: 978-5-7422-6498-9 DOI: 10.18720/spbpu/2/k19-116

EXPERIMENTS

Description of the diagnostic system

The data acquisition system from sensors of helium concentration is a matrix of sensor boards connected in a line with a serial interface. The sensor boards are composed of a microprocessor module based on the Atmega48 microcontroller, through which they communicate with a personal computer by the standard digital serial interface RS485 on one or two parallel twisted pair wires with a wave resistance of 120 Ohms. The interface baud-rate was selected as 57600. The information from the whole matrix of sensors was updated every 0.5 s. The communication protocol was MODBUS or special. The sensing element in the sensors is a gas thermal conductivity detector of TCG-3880 type pre-calibrated for helium individually for each sensor. The long-term calibration accuracy is 0.1 volume percent. This diagnostic system is described in more detail in [7].

Description of the experimental setup

The basis of the experimental setup was a rectangular frame made of metal beams, in the upper part of which a suspended ceiling of thick polyethylene membrane was stretched. The suspended ceiling had a height of 2.07 m and was placed in a wide closed room with ceiling height of 3 m. The length and width of the frame was 4.04 m. Helium was released vertically upwards in the exact center of the installation. After contacting the suspended ceiling, the flow spreads radially from the release axis forming an under-ceiling layer. After reaching the edges of the suspended ceiling, helium flowed up to the ceiling of the experimental room.

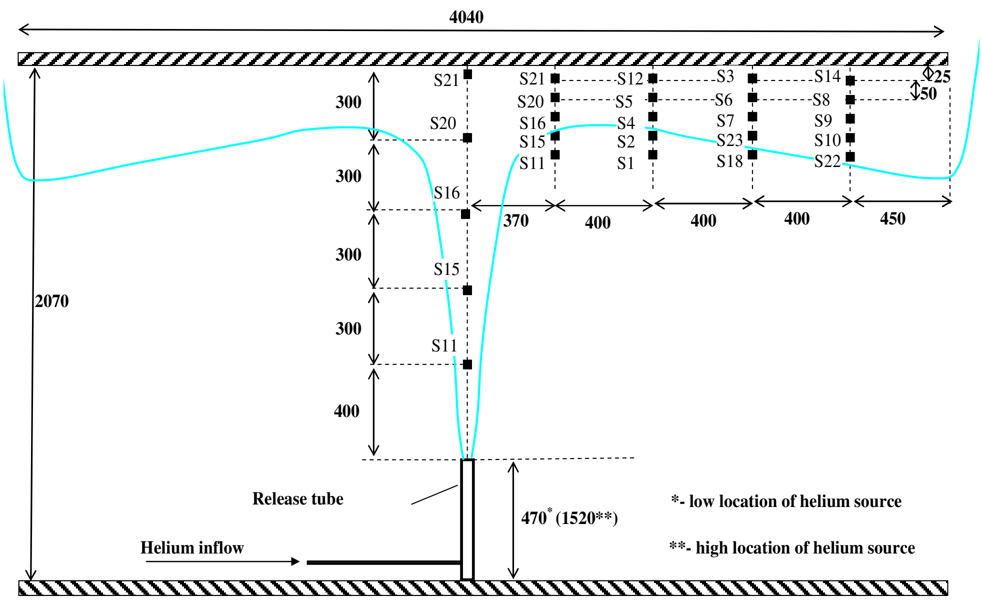

Fig. 1. Location of helium sensors relative to the up-flow axis and suspended ceiling.

The electronic sensor boards were fixed on a wooden plane along one of the spreading radiuses away from the axis and 1.5 m below the suspended ceiling. The helium sensor heads, which have a typical size of about 10 mm, were placed at certain distances from the boards on the shielded cables and fixed on four vertical threaded studs with a diameter of 8 mm by means of pairs of nuts with clamps moving along the studs. The scheme of their locations relative to the axis of the helium flow and the suspended ceiling is shown in Fig. 1 with the coordinates of all sensors. All dimensions are in millimeters. Sensors № 11, 15, 16, 20, 21 were used twice. Once in the general scheme when all sensor heads were located away from the axis. For the second time they were used to measure helium concentrations on the axis of the up-flow.

The difference between the jet and plume regimes of subsonic gas up-flow is the difference between the initial conditions of the gas release. If the initial momentum of the up-flow is large enough, then for the description of dynamics of a light gas one can neglect its buoyancy within some distance from the release point. However, it is clear that any vertical jet of light gas upon reaching some distance from the release point due to the action of buoyancy forces acquires an additional momentum which eventually surpasses the initial one, and the jet passes into the plume where the influence of the initial impulse is, as it were, forgotten. The length at which this occurs is called the plume formation distance. It is calculated for hydrogen by the formula [2, 8, 9]:

$$L_j = 0.32 v_0 \sqrt{D_0}\ , \tag{1}$$

In this formula D_0 is the initial diameter of the outflow, v_0 is the initial velocity of the outflow. For helium the numerical coefficient in this formula changes to 0.33. If the distance from the release point to the ceiling $H >> L_j$, the up-flow is plume type. If, on the contrary, the considered distances $H << L_j$, then the up-flow is jet type.

For realization of two main regimes of flowing – jet and plume – two different output pipes for vertical helium release were used. Both of them had a height of 470 mm, but the nozzle for jet flow was a narrow steel tube with inner diameter of 8 mm, and the nozzle for plume flow was a wide plastic pipe with an inner diameter of 98 mm. In the second case a metal mesh sponge was laid inside the wide pipe to equalize the gas flow in the cross section, and a disk of highly porous sponge metal was installed in the output section. The flowrates of helium in the experiments were from 5 to 16 l/s (i.e., from 0.89 to 2.85 g/s), and so the plume formation distance for jet modes were lying in the range 3 - 9 m, i.e., obviously greater than the height of the suspended ceiling, while for plume modes, in the range of 0.07 - 0.22 m, that is, certainly less than this height. These flowrates were chosen also to generate concentrations under the ceiling that would be reliably measurable with good accuracy and in accordance with the adopted level of hydrogen risk of the order of 4% and above. In eight experiments the injection pipes were lifted so that their outlets were at a height of 1520 mm above the floor to change the aspect ratio.

Experiments

Table 1 shows all the experimental runs carried out indicating the conditions of their realization and according to the sequence numbers.

The first two experiments were trials. All other experiments can be divided into two groups – experiments under the ceiling and experiments with the free up-flow of helium with the dismantled suspended ceiling and five sensors on the release axis – as shown in Fig. 1. The latter group includes four of the tests, №. 25-28. These experiments are connected with the two tests under the suspended ceiling, № 7 and 8, which also involved five sensors on the axis. These experiments were carried out to understand the effect of the ceiling on the change in helium concentration along the flow axis.

The main experiments under the ceiling differ in the type of up-flow (plume, jet), flowrate (5 and 16 l/s) and the height of the release point above the floor (470 and 1520 mm). All experiments with the same parameters were repeated two or three times.

RESULTS

The main experimental results are drawn out from the measurements of helium concentration dependencies in the periphery of the up-flow at distances from 25 to 225 mm from the suspended ceiling surface and from 370 to 1570 mm from the release axis. However, in tests №. 7, 8 and 25-28, measurements were made of the concentrations on the release axis by means of the five sensors placed 300 mm apart from each other (see Fig. 1). In these experiments the free up-flow was compared with the up-flow under the ceiling.

Table 1. Description of all experimental tests

№ test	Type of release	Release diameter, mm	Helium flowrate, l/s	Height of helium source, mm	Comment
3	jet	8	16	470	no sensors on axis
4	plume	98	16	470	no sensors on axis
5	plume	98	16	470	no sensors on axis
6	plume	98	16	470	no sensors on axis
7	jet	8	16	470	5 sensors on axis
8	plume	98	16	470	5 sensors on axis
9	plume	98	5	470	1 sensor on axis in top point
10	plume	98	5	1520	1 sensor on axis in top point
11	plume	98	5	1520	1 sensor on axis in top point
12	plume	98	16	1520	1 sensor on axis in top point
13	plume	98	16	1520	1 sensor on axis in top point
14	jet	8	5	1520	1 sensor on axis in top point
15	jet	8	5	1520	1 sensor on axis in top point
16	jet	8	16	1520	1 sensor on axis in top point
17	jet	8	16	1520	1 sensor on axis in top point
18	jet	8	5	470	1 sensor on axis in top point
19	jet	8	5	470	1 sensor on axis in top point
20	jet	8	16	470	1 sensor on axis in top point
21	jet	8	16	470	1 sensor on axis in top point
22	plume	98	5	470	1 sensor on axis in top point
23	plume	98	5	470	1 sensor on axis in top point
24	plume	98	16	470	1 sensor on axis in top point
25	plume	98	16	470	without ceiling, 5 sensors on axis
26	jet	8	16	470	without ceiling, 5 sensors on axis
27	jet	8	5	470	without ceiling, 5 sensors on axis
28	plume	98	5	470	without ceiling, 5 sensors on axis

In each experiment the reducer on the gas cylinder was used to set a constant flowrate on the calibrated differential pressure gauge which was maintained for 25-30 seconds. At this time there was an automatic recording of the readings of all sensors with the help of the described above digital data collection system directly to a personal computer, where the data for each experiment were stored as a file.

On the basis of these stationary readings, two main experimental values were calculated – the thickness of the under-ceiling layer and the decay in the under-ceiling concentration along the radius from the release axis. The thickness of the under-ceiling layer was calculated on each of the four vertical sensor lines, which were 370, 770, 1170, and 1570 mm away from the flow axis (see

Fig. 1). The sensors on each of these vertical lines were spaced from the ceiling by 25, 75, 125, 175, and 225 mm. The concentration values at these points of the experimental dependences can be approximated by the Gauss curve $A\exp\left(-z^2/h^2\right)$ by regression method with two parameters for the smallest sum of squared deviations. In this case z characterizes the distance from the ceiling, A is the first regression parameter characterizing the maximum value of the concentration directly under the ceiling, while h can be interpreted as the characteristic thickness of the under-ceiling layer of helium spreading along the ceiling at a given radius from the release axis of the up-flow. This is a calculated value and it will be used further as an estimate of the characteristic thickness of the under-ceiling layer.

In Fig. 2 the data from five near-ceiling sensors collected in the experiments, № 3, 12, 14, 16 and 21, are shown including sensor № 21 directly on the release axis. According to these data, an average value was calculated for the signal of each sensor at the time of reaching the stationary readings by all sensors.

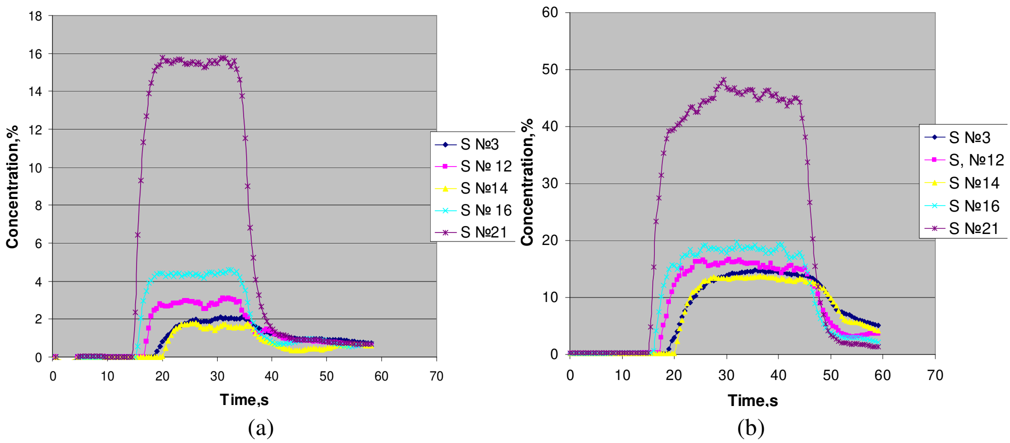

Fig. 2. Concentration versus time on the near-ceiling sensors № 21, 16, 12, 3, and 14: (a) – experiment №16, jet; (b) – experiment №12, plume.

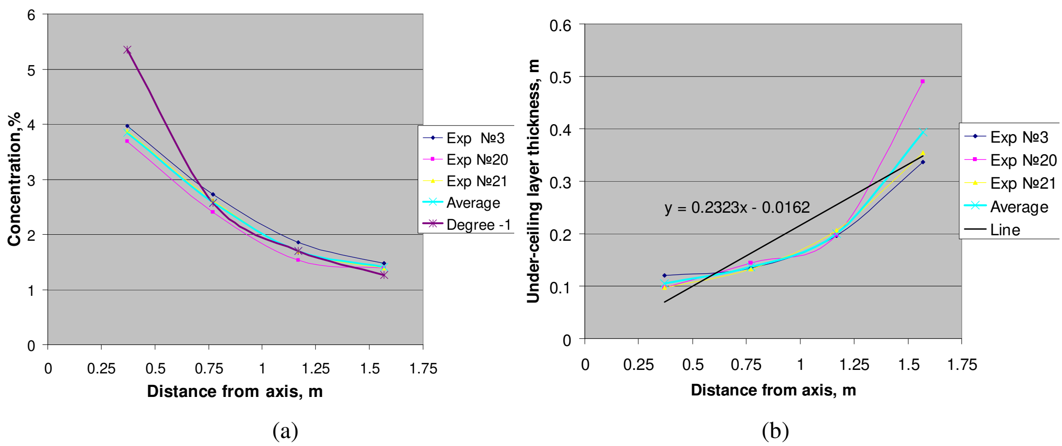

Fig. 3. Experimental dependences of under-ceiling concentration and layer thickness at the distance r from the flow axis. Jet regime, helium flowrate 16 l/s, release point is 470 mm above the floor. (a) – Concentration decline ~ r^{-1}; (b) – Linear approximation of the layer thickness growth has a slope of 0.2323.

In Fig. 3 the specified dependences of the decrease in the under-ceiling concentration and the thickness of the under-ceiling layer for the experiments in the jet regime at helium flowrate of 16 l/s and the height of the release point above the floor of 470 mm are presented. The results of three similar experiments of № 3, 20 and 21 are presented as well as the average value. For all the experiments with the same parameters, the average value at each point was determined and a corresponding average curve was constructed.

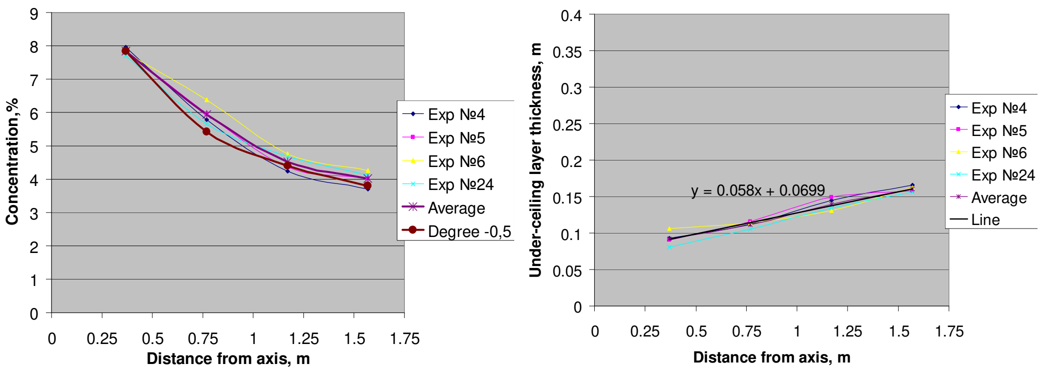

(a) (b)

Fig. 4. Experimental dependences of under-ceiling concentration and layer thickness at the distance r from the flow axis. Plume regime, helium flowrate 16 l/s, release point is 470 mm above the floor. (a) – Concentration decline ~ $r^{-0.5}$; (b) – Linear approximation of the layer thickness growth has a slope of 0.058.

For the approximation of the decrease rate of the under-ceiling concentration with distance from the release axis the power-law dependences of the type $r^{-\alpha}$ were chosen, where r is the distance from the release axis. This approximation was made for average values of the dependences obtained in three similar experiments. In this case, the approximation was carried out in such a way that the concentration values in it and in the experiment at a distance of 770 mm from the flow axis coincide. From Fig. 3a one can see that, for the given parameters of the experiment, the last three most remote points from the flow axis, which characterize the decline of the concentration on the radius r, fit very well to the dependence r^{-1}.

The thickness of the under-ceiling layer grows quite rapidly with distance from the release axis. If it is approximated by a linear approximation, the slope coefficient is quite large and is equal to 0.2323 (Fig. 3b).

Figure 4 shows the dependences of the under-ceiling concentration and layer thickness on the distance from the release axis for the same flowrate of 16 1 / s and the same height of the release point as in Fig. 3, but for the plume regime. The decline in the near-ceiling concentration on the upper sensors is significantly slower than in Fig. 3 and is well approximated by the dependence $r^{-0.5}$. The thickness of the layer also grows significantly slower than in the jet regime with the same flowrate.

In Fig. 5, data similar to those in Fig. 4 for the jet regime with the height of the release point above the floor of 470 mm are shown, but for the smaller flowrate of 5 l/s. It can be seen that the rate of decay of the concentration with a decrease in the flowrate slowed to $r^{-0.75}$ and, at the same time, the growth of the layer thickness with distance from the release axis also became slower. It should be noted that a significant (3.2 times) decrease in helium flowrate did not lead to any significant decrease in the concentration on the near-ceiling sensors in comparison with the data in Fig. 3.

In Fig. 6 the dependences of the concentration and under-ceiling layer thickness are depicted for the same flowrate of 5 l/s and the same height of the release point of 470 mm as for Fig. 5, but for the plume regime. The dependencies are almost the same as for the plume data in Fig. 4 with a flowrate of 16 l/s: the same degree $r^{-0.5}$ reflecting the rate of decay of the under-ceiling concentration and almost the same slope angle of the linear approximation. The total concentration level at each point is about two times lower than in Fig. 4 for a flowrate of 16 l/s. Thus, in contrast to the jet regime, a decrease in the volume flowrate at the release point by 3.2 times in case of the plume regime led to a decrease in the near-ceiling concentrations by about a factor of two.

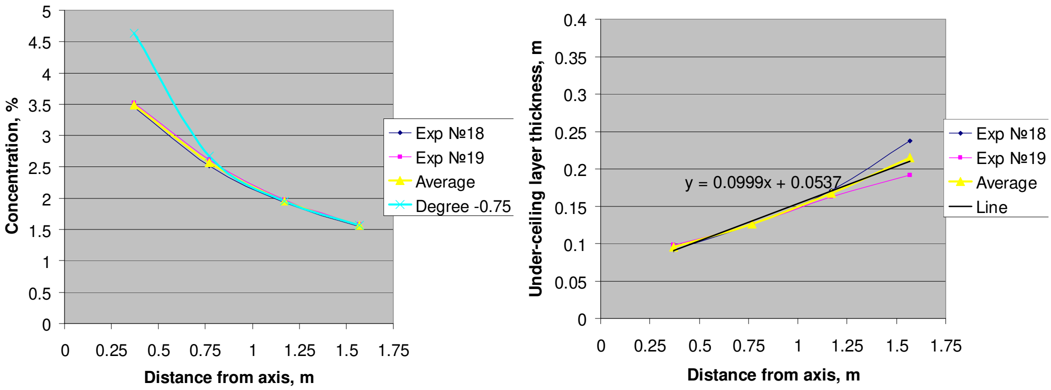

(a) (b)

Fig. 5. Experimental dependences of under-ceiling concentration and layer thickness at the distance r from the flow axis. Jet regime, helium flowrate 5 l/s, release point is 470 mm above the floor. (a) – Concentration decline ~ $r^{-0.75}$; (b) – Linear approximation of the layer thickness growth has a slope of 0.1.

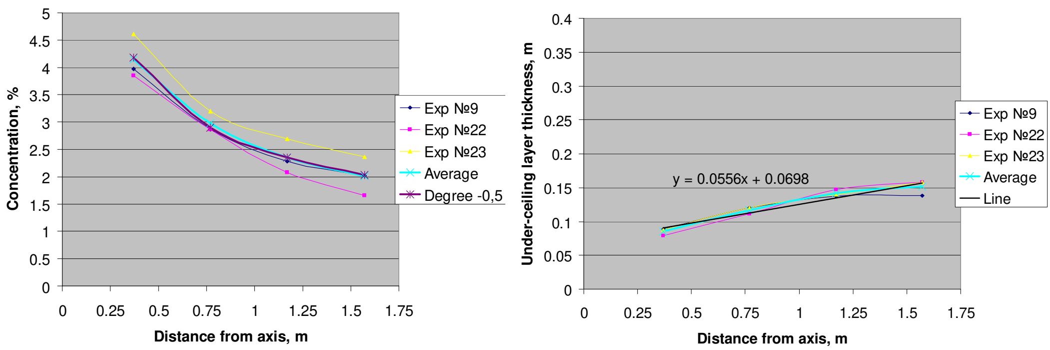

(a) (b)

Fig. 6. Experimental dependences of under-ceiling concentration and layer thickness at the distance r from the flow axis. Plume regime, helium flowrate 5 l/s, release point is 470 mm above the floor. (a) – Concentration decline ~ $r^{-0.5}$; (b) – Linear approximation of the layer thickness growth has a slope of 0.056.

The experiments where the release point was raised to a height of 1520 mm above the floor are presented starting from Fig. 7. This mode is particularly interesting because it increases the aspect ratio of the available length of the ceiling from the edge to the release axis (2 m) with respect to the distance from the ceiling to the release point (0.55 m) up to almost 4.

In Fig. 7 the data on the jet up-flow under the ceiling from the height of 1520 mm above the floor at the flowrate of 16 l/s in two experiments are presented. The difference with the experimental conditions shown in Fig. 3 is only in the height of the release point. As it can be seen from Fig. 7, the raising of the release point introduced no significant difference. There is the same rate of decline in the under-ceiling concentration ~ r^{-1}. The growth rate of the under-ceiling layer thickness is about the same, with a slope coefficient of 0.21. Also, the initial value of the thickness of the under–ceiling layer on the nearest to the axis vertical line of sensors is almost 2 times less – only 0.06 m.

Figure 8 presents the experiments in the plume regime of up-flow with the same experimental conditions shown in Fig. 4 except for raising the release point to 1520 mm above the floor. This mode is characterized by a significant difference in the rate of decline of the near-ceiling concentration – it significantly slows down and its asymptotic is well described by the dependence ~ $r^{-0.25}$.

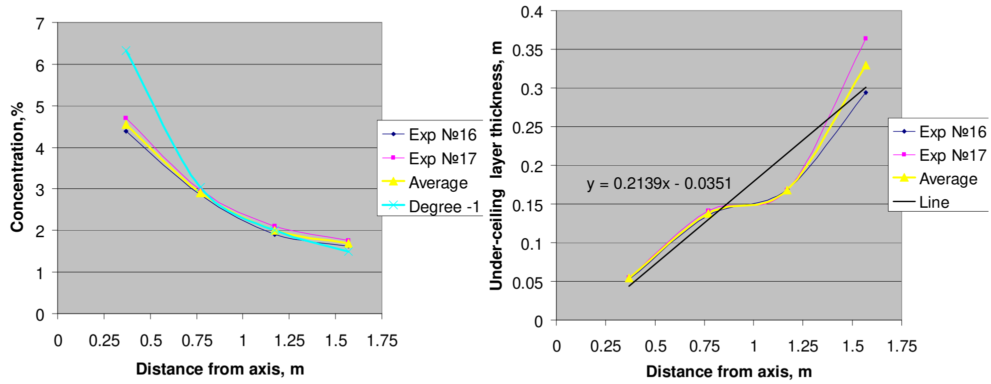

(a) (b)

Fig. 7. Experimental dependences of under-ceiling concentration and layer thickness at the distance r from the flow axis. Jet regime, helium flowrate 16 l/s, release point is 1520 mm above the floor. (a) – Concentration decline ~ r^{-1}; (b) – Linear approximation of the layer thickness growth has a slope of 0.21.

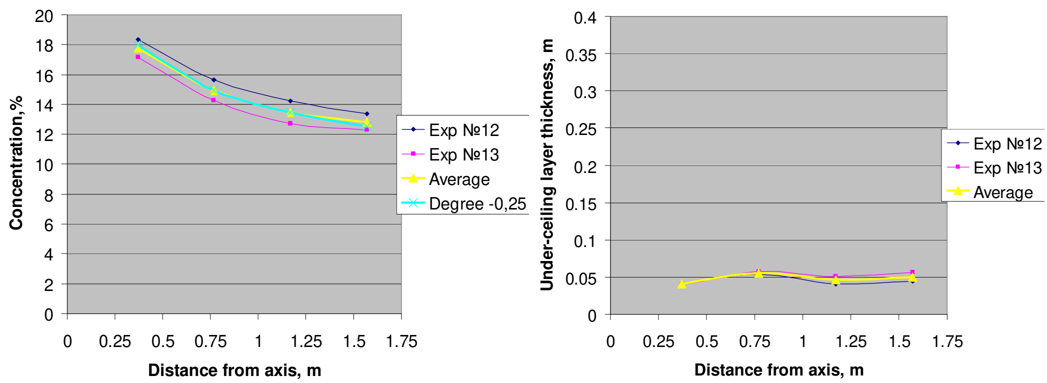

(a) (b)

Fig. 8. Experimental dependences of under-ceiling concentration and layer thickness at the distance r from the flow axis. Plume regime, helium flowrate 16 l/s, release point is 1520 mm above the floor. (a) – Concentration decline ~ $r^{-0.25}$; (b) – Thickness of the layer practically does not increase with distance from release axis.

At the same time this is accompanied by the fact that the thickness of the under-ceiling layer practically ceases to grow with distance from the release axis, its value is 0.05 m at any available radius of the experiments, while at the release from the position of 470 mm above the floor (Fig. 4b) this thickness began to grow with a value of 0.1 m with a slope of 0.058. The total values of the near-ceiling concentrations significantly increase in comparison with Fig. 4. It is obvious that this experimentally detected feature of the plume flow regimes should directly lead to a sharp increase in the volume of the flammable hydrogen-air mixture in the under-ceiling spreading layer in comparison with the jet regime with the same flowrate in Fig. 7.

The experiments, carried out with the sensors on the release axis in case of the suspended ceiling and without it, showed that the concentration at the upper under-ceiling sensor in the plume regime exceeds that in the jet regime with the same flowrate 16 l/s by 2.4 times in case of the ceiling and by 1.9 times in its absence. So, the much slower decrease in the concentration in the plume regime in the under-ceiling layer along the radius from a larger initial concentration leads to the formation of an extended area of flammable volume (where the concentration exceeds 4%) in the form of a flat pancake directly under the ceiling. In the jet regime, with a rapid decline of under-ceiling concentration along the radius from a smaller initial value, the area of flammable concentration occupies an insignificant volume mostly near the release axis.

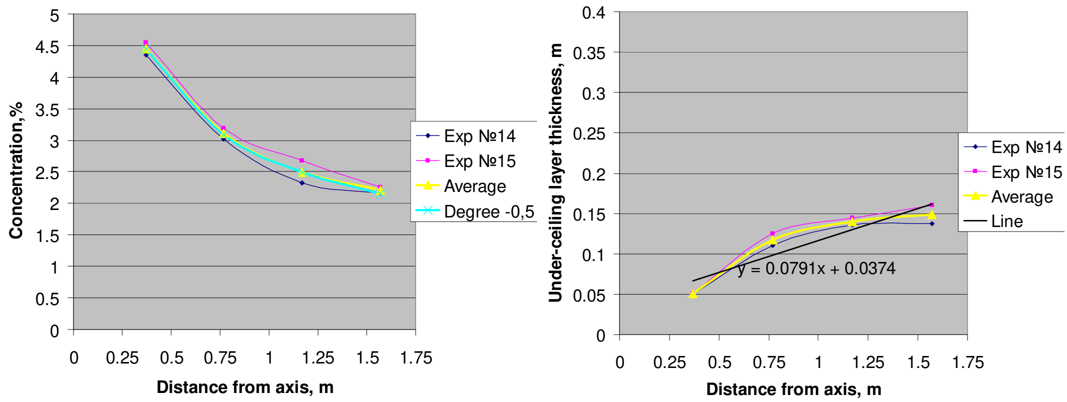

(a) (b)

Fig. 9. Experimental dependences of under-ceiling concentration and layer thickness on the distance r from the flow axis. Jet regime, helium flowrate 5 l/s, release point is 1520 mm above the floor. (a) – Concentration decline ~ $r^{-0.5}$; (b) – Linear approximation of the layer thickness growth has a slope of 0.08.

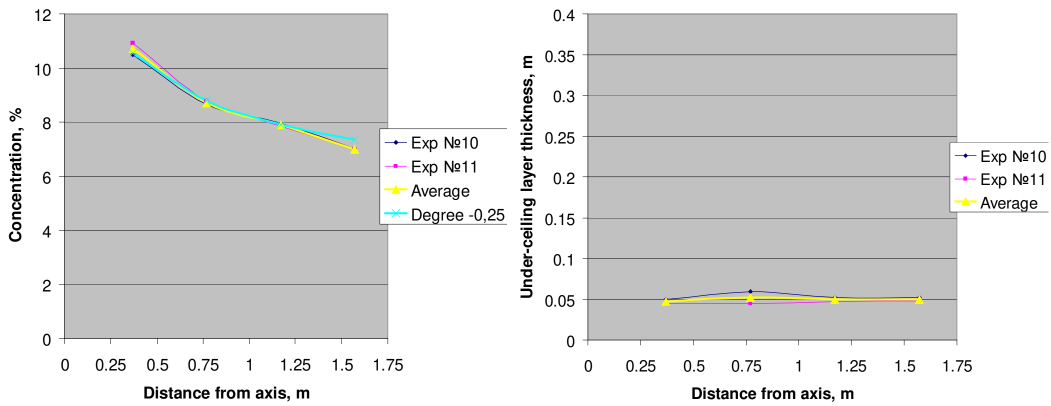

(a) (b)

Fig. 10. Experimental dependences of under-ceiling concentration and layer thickness at the distance r from the flow axis. Plume regime, helium flowrate 5 l/s, release point is 1520 mm above the floor.

(a) – Concentration decline ~ $r^{-0.25}$; (b) – Thickness of the layer practically does not increase with distance from release axis.

In Fig. 9 one can see the dependences of the concentration and the under-ceiling layer thickness on the distance from the release axis in the experiments in the jet regime at helium flowrate of 5 l/s and the height of the release point of 1520 mm above the floor. The decline in the near-ceiling concentration here is the slowest for all the considered jet flow regimes and is characterized by a rate ~ $r^{-0.5}$ – just like for plume regimes with the release point height of 470 mm. Also, the average slope of the linear approximation of the layer thickness growth is sufficiently small.

Figure 10 presents the experiments in the plume regime similar by conditions to those shown in Fig. 8 but with the small flowrate of 5 l/s. The type of dependence has the same remarkable characteristics from the point of view of fire risk as in Fig. 8: slow rate of concentration decline ~ $r^{-0.25}$ and constant thickness of the under-ceiling layer at any distance from the flow axis within the sensor locations. The lower flowrate leads to smaller levels of concentration but did not affect the thickness of the under-ceiling layer which remained equal to 0.05 m.

ANALYSIS

Figure 11 shows the relative boundaries of the jet and plume up-flows at the interaction with the ceiling. The boundaries of the jet and the plume at the vertical up-flow from the corresponding nozzle are constructed on the basis of the standard opening angle of the turbulent jet α, lying in the range 12-14° and determined by the coefficient of turbulent entrainment of ambient air. The relative boundaries of the layer lying under the ceiling in both cases are shown on the assumption of above-described features of the change in the thickness of the under-ceiling layer revealed in the experiments. The main feature of the jet outflow at the high flowrate of 16 l/s is that the angle formed by the boundary of the spreading under-ceiling layer at the interaction with the ceiling and the ceiling plane (angle β in Fig. 11) is sufficiently large and numerically approximately equal to the opening angle of the turbulent jet α (tan β ≈ 0.23 – see Fig. 3 and 7). In case of the smaller flowrate of 5 l/s, the tangent of the angle β decreases to 0.1, and there is a tendency to slow the growth rate of the thickness of the ceiling layer with distance from the axis (dotted line in Fig. 11) in case of approach to the ceiling of the release point of the jet up-flow.

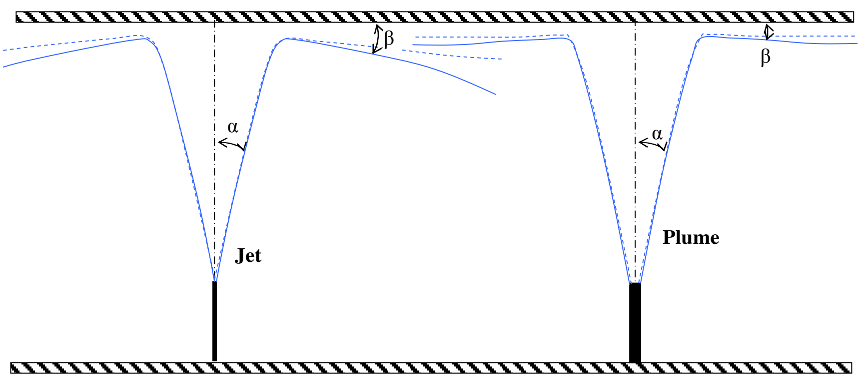

Fig. 11. The characteristic shape of the jet and plume at interaction with the ceiling**.**

In the jet regimes, the under-ceiling concentration falls quite rapidly with distance from the release axis: in case of a large flowrate the asymptotic decline behaves as ~ r^{-1} at any height of the release point, while a reduction in the volumetric flowrate in the jet leads to a slower rate of decline in the under-ceiling concentration from ~ $r^{-0.75}$ (at a lower position of the release point) to ~ $r^{-0.5}$ when approaching the release point to the ceiling. This results in a very small volume of flammable hydrogen-air mixture concentrated mainly near the release axis.

The plume regimes are characterized by a small angle of reflection from the ceiling β at the spreading of the under-ceiling layer in case of a lower position of the release point both at a large and small flowrate ($\tan\beta \approx 0.05$-0.06). In this case the approximation of decay in the near-ceiling concentration is fitted well by the slow dependence ~ $r^{-0.5}$. In the case where the release point is moved closer to the ceiling, the plume regimes both with small and large volume flowrates produce a layer under the ceiling whose thickness practically does not change as it moves away from the axis of the plume. In this case, the asymptotic decay in the near-ceiling concentration is well described by a very slow dependence ~ $r^{-0.25}$. This leads to the formation of an extended flat area under the ceiling in the form of a pancake, in which flammable concentrations of hydrogen are present at large distances from the release axis.

There is a clear correlation between the angle of reflection of the gas flow from the ceiling β and the rate of decrease of the near-ceiling concentration along the radius. It looks like a decrease in the rate of decay of the near-ceiling concentration as the angle of reflection β decreases in all regimes - jet and plume.

We can try to apply the conservation equations to the stationary state of gas motion in the under-ceiling layer to analyze the experimental results. To do this, we assume that within its characteristic thickness h the layer moves with the same average velocity v, and outside h there is no movement. The real profile of the volume concentration of light gas in the layer C is also replaced by a rectangular one with the same thickness h. At any radius r remote from the release axis by a sufficient distance for a vertical flow to pass into the creeping under-ceiling layer, the same number of light gas particles must pass through the ring vertical cross-section of the layer with an area of $2\pi rh$ per time unit. This enforces conservation of mass of injected material. Hence, we have the first integral of stationary motion of the buoyant under-ceiling layer:

$$Cvrh = const \,. \tag{2}$$

The second integral can be obtained under the assumption that the friction of the moving layer on the ceiling can be neglected. In the case of its applicability there is a law of conservation of the radial momentum in the layer. Neglecting the slow change in the density of the gas mixture in the layer as it spreads over the radius, we obtain the second integral of motion:

$$rhv^2 = const \,. \tag{3}$$

Combining Eqs. (2) and (3) we get:

$$v(r) = const \cdot C(r) \,, \tag{4}$$

and

$$C^2(r)\, r\, h(r) = const \,. \tag{5}$$

For jet release regimes, as was found above, the growth of the under-ceiling layer thickness is according to the law $h(r) = r\mathrm{tg}\beta$ (see Fig. 11). Substituting this expression in Eq. (5) we obtain that the concentration in the layer should fall according to the law $C = const \cdot r^{-1}$, which in general was observed in the experiments for jet regimes of up-flow. Besides, it follows from Eq. (4) that the average radial velocity in the under-ceiling layer is subject to the same dependence. This result is in good agreement with the data of reference [10], where a turbulent radial wall jet formed by an impinging circular jet on a smooth flat plate was investigated. For plume release regimes characterized by a small increase in the thickness of the under-ceiling layer with radius or no such growth, substituting $h = const$ in Eq. (5), we obtain $C = const \cdot r^{-0.5}$, while for plumes with a constant thickness of the under-ceiling layer a slower dependence $C = const \cdot r^{-0.25}$ is observed experimentally. This means that for jet flow regimes characterized by a large initial momentum friction against the ceiling can be neglected at least at some distance from the jet axis (in experiments up to the edge of the suspended ceiling), because the application of conservation of momentum (Eq. (3)) gave a rate of concentration decay in the layer consistent with the experiment. While for plume flow regimes characterized by a low initial momentum it is obvious that the application of Eq. (3) is too strong an assumption, and therefore the friction against the ceiling cannot be neglected.

Thus, while deriving the theoretical dependences of the parameters of the flowing under-ceiling layer at the interaction of a vertical jet and plume with the ceiling, we can now conclude that for jets the friction on the ceiling (at least up to a certain distance from release axis) can be neglected, while for plumes it cannot be. Weak jets (with a small initial flowrate) while interacting with the ceiling behave similar to the plumes with a lower point of release, according to the characteristic dependencies of their under-ceiling layers. This leads to the conclusion that the key parameters characterizing the interaction of the vertical flow of a light gas with the ceiling are the value of the initial momentum and the distance to the ceiling from the release point of the gas.

CONCLUSION

The results of the experiments and their analyses clearly demonstrate that the two modes of hydrogen release – plume and jet – can produce at the same flowrate radically (perhaps by orders of magnitude) different flammable volumes in case of a sufficiently long release of hydrogen under an extended ceiling.

The experiments were carried out at moderately high flowrates of helium (hydrogen substitute) > 1 g/s, which can be considered as a conservative estimate for hydrogen outflows from the fuel tanks of hydrogen cars in garages and closed parking lots with an extended ceiling. It was found that the most dangerous leakages are those that generate plume (not jet) release regimes of formation of flammable hydrogen-air clouds. At the same flowrate of hydrogen leakage, the volumes and masses of flammable hydrogen-air mixtures can increase manifold due to a principally different character of interaction with extended ceilings in plume regimes compared with jet regimes. Thus, the influence of the release momentum of hydrogen leakage, as well as the distance from the leakage point to the ceiling are fundamental for hydrogen safety.

The correlations of concentration fields of light gas under the extended ceiling depending on the different release regimes obtained in conditions of a direct experiment modeling of real hydrogen leaks can be used to specify rules of hydrogen safety for parking of hydrogen cars, as well as for industrial and infrastructure facilities where hydrogen is used.

REFERENCES

[1] M.R. Swain, P. Filoso, E.S. Grilliot, M.N. Swain, Hydrogen Leakage into Simple Geometric Enclosures, Int. J. Hydrogen Energy 28 (2003) 229-248.

[2] R. Zalosh, Hydrogen Mixing in Large Enclosures, HYSAFE Lecture, University of Ulster, 2006.

[3] S. Benteboula, A. Bengaouer, B. Cariteau, Comparison of Two Simplified Models Predictions with Experimental Measurements for Gas Release within an Enclosure, In: ICHS2009, Ajaccio – Corsica, 2009, ID 226.

[4] V.P. Denisenko, I.A. Kirillov, S.V. Korobtsev, I.I. Nikolaev, Hydrogen-Air Explosive Envelope Behaviour in Confined Space at Different Leak Velocities, In: ICHS2009, Ajaccio – Corsica, 2009, ID 194.

[5] V.P. Denisenko, I.A. Kirillov, S.V. Korobtsev, I.I. Nikolaev, Hydrogen Distribution in Enclosures: on Distinction Criterion between Quasi-Homogeneous Mixing and Stratification Modes, In: ICHS2013, Brussels, 2013, ID 170.

[6] S. Jallais, Build-up in Unventilated Rooms and Enclosures with One and Two Vents: Engineering Point of View, In: Hyindoor Research WorkShop, Brussels, 2013.

[7] V.P. Denisenko, I.A. Kirillov, S.V. Korobtsev, I.I. Nikolaev, A.V. Kuznetsov, V.A. FeldStein, V.V. Ustinov, Experiments on Subsonic Release and Propagation of Hydrogen in Closed Cylindrical Volume. Empirical Analysis, J. Fire Saf. 2 (2011) 38-46 (in Russian).

[8] B.R. Morton, Forced Plumes, J. Fluid Mech. 5 (1959) 151-163.

[9] W.D. Baines, J.S. Turner, Turbulent Buoyant Convection from a Source in a Confined Region, J. Fluid Mech. 37 (1969) 51-80.

[10] M. Poreh, Y.G. Tsuei, J. E. Cermak, Investigation of a Turbulent Radial Wall Jet, Trans. ASME, J. Appl. Mech. 34 (1967) 457–463.